ESTIMATION OF VULNERABLE AREA IN KANGWONDO USING 2-PASS DINSAR TECHNIQUE

Jae-Hoon Jung*, Hong-Gyoo Sohn**, Kong-Hyun Yun***

*lionheart_kr@yonsei.ac.kr, **sohn1@yonsei.ac.kr, ***ykh1207@yonsei.ac.kr
Geomatic & GSIS Lab. College of Engineering
Yonsei University, Seoul, Korea
Tel: 82-2-2123-2809

ABSTRACT: Korea Peninsula is exposed to landslide problems because large regions of Korea are composed of mountain. As a result, we have a great loss of life and property every year, such as road, bridge, and building. However, conventional survey has many restrictions of time and man power. In recent days, instead of field surveying, remote sensing has our attention for detecting damaged place. Synthetic Aperture Radar (SAR) provides the all-weather capability and complements information available. And through the 2-pass DInSAR technique, we can measure even very small displacement effect. In this study, we generated six interferograms of Kangwondo between 1992 and 1998, and estimated the vulnerable place for landslide.

KEY WORDS: SAR, DEM, Interferometry, 2-pass DInSAR,

1. INTRODUCTION

In recent days, climatic change cause abnormal weather all over the world and we have a great loss of life and property every year. In Korea, we suffer from landslide problem because large regions of Korea Peninsula are composed of mountain. Rapid detection and to take follow-up measures of disaster, the remote sensing is being used actively in many countries as conventional field survey has many restrictions in accessibility because of more time and man power requirement. And Interferometric SAR is one of the techniques that have our attention because it could provide many kinds of accurate surface information without restriction of atmospheric and ground conditions. .

Synthetic Aperture Radar (SAR) is an active, imaging method based on microwaves which is used on mobile platforms such as aeroplanes or satellites. Compared to real aperture radar which needs a huge antenna to get the high resolution, SAR virtually increases the antenna's size for azimuth direction by intergration of the back scattering signal and in opposition to passive methods deployed in the optical and short-wave infrared sector that image an area by means of reflected sunlight, SAR allows unrestricted service irrespective of solar radiation and daytime. Furthermore it is possible to choose the transmitted wave length in such a way that the attenuation of electromagnetic waves caused by the atmosphere can be disregarded. Thus, the SAR sensor can be operated under almost any weather conditions and is able to even observe an area deep in clouds.

Interferometric SAR (InSAR) is the process extracting information from the phase data. If two observations of the same region from very similar position are available, aperture synthesis can be performed to provide the resolution performance which would be given by a RADAR system with dimensions equal to the separation of the two measurement.

If the two samples are obtained simultaneously by two antennas on the same aircraft, some distance apart, then the phase difference can contain the information about the angle from which the radar echo returned. Combining this with the distance information, we can get the position in the three dimensions of the image pixel. i.e. we could extract terrain altitude as well as radar reflectivity, producing a digital elevation model (DEM).

In case two samples are separated in time by two flights covering the same terrain, there are two kinds of phase shift available, terrain altitude and motion. If the terrain has shifted between observations, it will return a different phase and the amount of shift can be seen by the order of the wavelength used.

The interferometric phase is sensitive to both, surface topography and coherent displacement in between the acquisition of an image pair. The basic idea of differential interferometric processing is to separate the two effects and retrieve a differential displacement map. This goal may be achieved by subtracting the topography related phase. The topography related phase can either be calculated from a conventional DEM or from an independent interferometric pair without phase component from differential displacement. There are three kinds of common methods in differential interferometry, 2-pass, 3-pass, and 4-pass. In this study, we aimed to estimate the vulnerable mountain area for landslide by 2-Pass DInSAR. The principles are as the following.

2. PRINCIPLES OF 2-PASS DINSAR

2-pass differential interferometry (2-pass DInSAR) is based on an interferometric image pair and a Digital Elevation Model (DEM). The DEM may either be given in a map projection, or in the slant range-azimuth geometry of the SAR image.

The basic idea of 2-pass DInSAR is that a reference interferogram which has the phase corresponding to surface topography is simulated from the DEM. For this process, the DEM is transformed from its original coordinate system to the reference SAR image coordinate. This is done in two steps. First, the geometric transformation is done based on the available information on the geometry of the DEM and the SAR image geometry used. In the same step the SAR image intensity is simulated based on the simulated local pixel resolution and incidence angle. Inaccurate DEM coordinates, orbit data, and small errors in the calculation of the geometric transformations could make a small offsets between the real SAR image and the simulated image geometry. In the next step the offsets between the real and simulated image intensities are estimated and used to accurately register the transformed DEM to the SAR image geometry.

Based on the reference SAR geometry, the interferometric baseline model, the transformed height map, and the unwrapped interferometric phase corresponding exclusively to topography is calculated. This also be called topographic phase and may either be subtracted from the complex interferogram (resulting in a complex differential interferogram) or unwrapped phase (resulting in the unwrapped differential phase). Figure 1 shows the flowchart of 2-pass DInSAR process.

Subtracting the latter from the reference interferogram can reveal differential fringes, which are a result of SAR range changes of any displaced point on the ground from one interferogram to the next. In the differential interferogram, each fringe is directly proportional to the SAR wavelength, which is about 5.6 cm for ERS, RADARSAT (C-band) and 23.5 cm for JERS-1 (X-band) single phase cycle. Surface displacement away from the satellite look direction causes an increase in path (translating to phase) difference. Since the signal travels from the SAR antenna to target and back again, the measured displacement is twice the unit of wavelength. This means in differential interferometry one fringe cycle –pi to +pi or one wavelength corresponds to a displacement relative to SAR antenna of only half wavelength (2.8 cm and 11.7 cm each).

There are Envisat, JERS, and LADARSAT that InSAR technology can be applied. The research site, Kangwondo has many forest areas, so coherence is a critical issue. To get sufficient coherence, it is more appropriate to utilize L-band than C-band, because it has high Signal to Noise ratio.

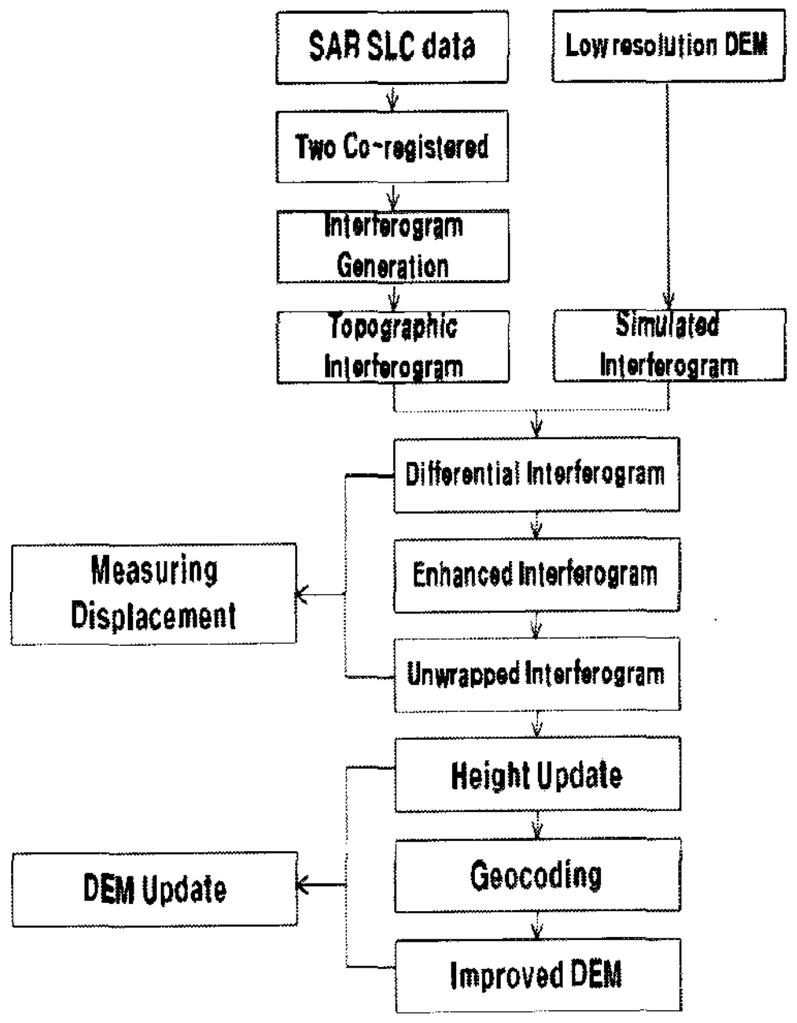

Figure 1. Flow chart of 2-pass DInSAR

3. 2-PASS DINSAR PROCESSING IN KANGWONDO

Kangwondo is a province located in eastern part of Korea Peninsula. Most areas in Kangwondo are composed of mountain, so it is exposed to serious landslide problems every year. In this research, we aimed to estimate the vulnerable mountain area for landslide in Kangwondo by using 2-pass DInSAR technique. For this, we selected two sites, around Sokcho city (N : 38.12, E : 128.33) and Gangneung city (N : 37.45, E : 128.54) as seen in Figure 2.

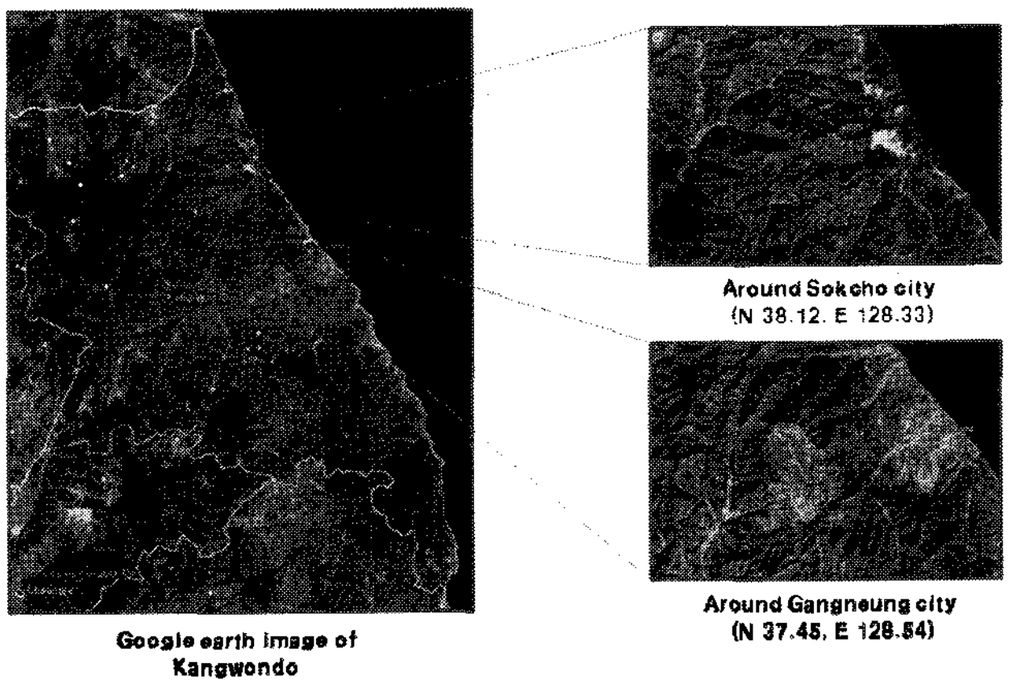

Figure 2. Objective sites for 2-pass DInSAR

For differential interferometric approach, a SAR image pair and a DEM (in map coordinates) are required. Six interferograms of research area were prepared from JERS-1 SAR dataset between 1992 and 1998, (Table 1.) and simulated topographic phase were generated from

DEM. Then, subtracting simulated phase from interferometric phase and the differential phase was obtained about displacement of target area. The results are as the followings. The displacement areas are expressed by red or yellow color. (Figure 3.)

Table 1. JERS-1 data for objective sites

Area	JERS-1		Number
Sokcho (N 38.12, E 128.33)	Master	Slave	
	930727	930909	①
	971127	980110	②
	980705	980818	③
Gangneung (N 37.45 E 128.54)	960730	961026	④
	970830	971013	⑤
	980704	980817	⑥

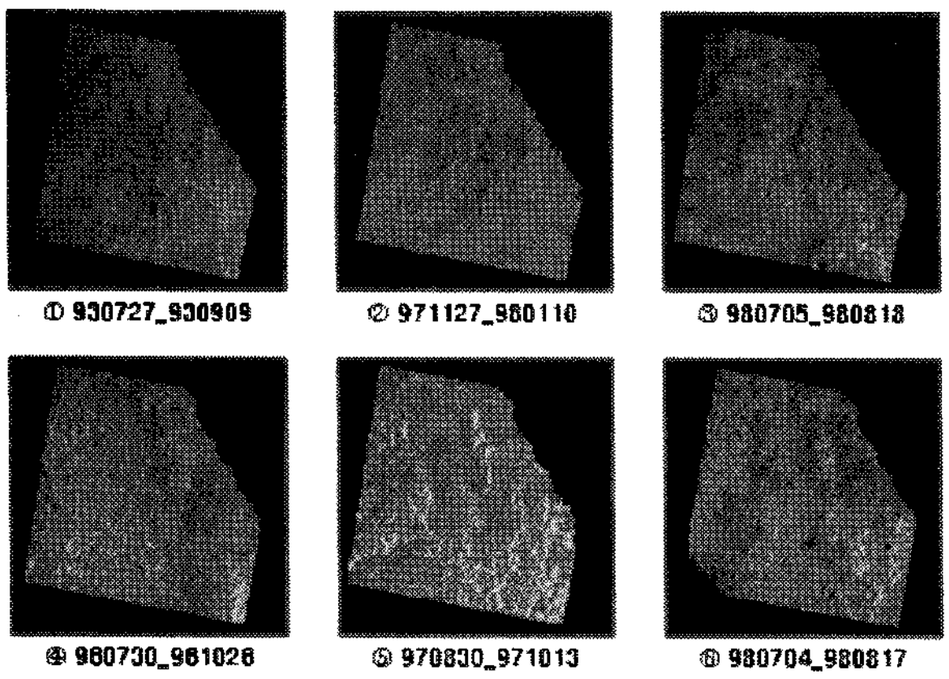

Figure 3. Displacement images for objective sites

The displacement image ①, ②, ④ show better result than others because displacement image ③, ⑤, ⑥ have long baseline. Interferograms are generated from two single look complex (SLC) images of the same region and the perpendicular distance between the different satellite positions is baseline. Table 2. show the baselines of each interferograms.

Table 2. Baseline of each interferograms

Image	Baseline (m)	Number
930727_930909	375.3378996	①
971127_980110	347.7937810	②
980705_980818	1675.2080922	③
960730_961026	-145.0738172	④
970830_971013	-1722.6835948	⑤
980704_980817	1419.8699093	⑥

The phase accuracy of SAR interferograms is mainly affected by baseline decorrelation which occurs when the interferometric baseline is not exactly zero. The baseline decorrelation is related to the different look angles of the two SAR acquisition, and leads to a critical baseline. For JERS-1, the baseline which is longer than about 1 km cause many errors for generating interferogram. As seen in table 2, baselines of interferogram ③, ⑤, ⑥ are much longer than the limit and actually, these interferograms show unreasonable displacement data. We also excluded the interferogram ④ because no other interferograms exist for comparison in Gangneung. So, we only used two interferograms (①, ②,) to estimate the vulnerable areas in Kangwondo. And we emphasized this regions by yellow color line. (Figure 4.)

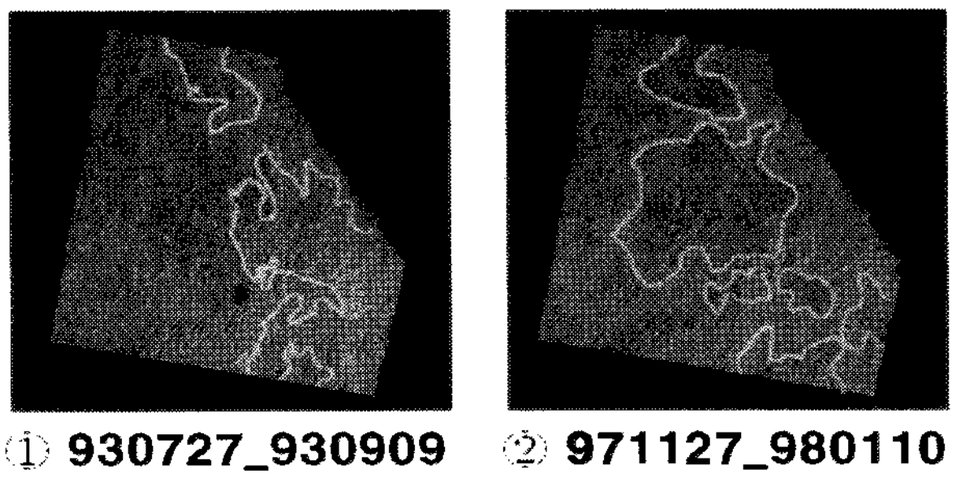

Figure 4. Displacement areas of different period

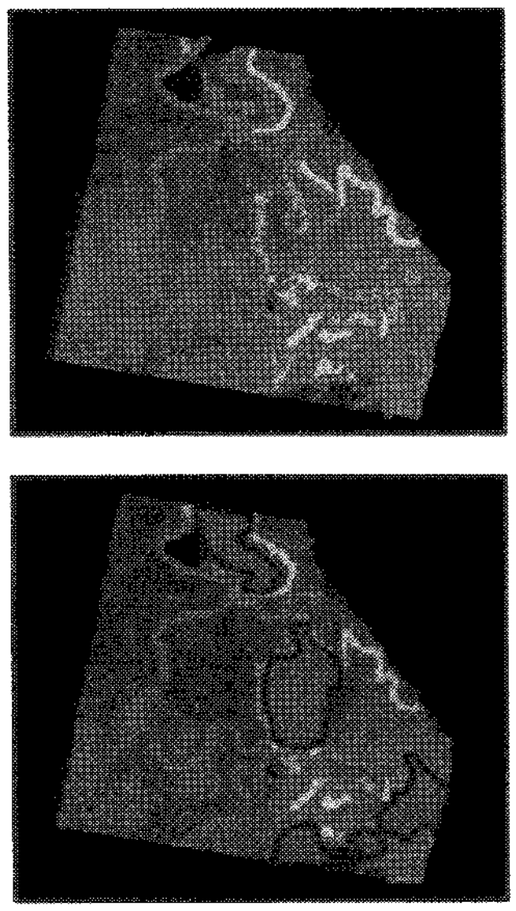

Figure 5. The vulnerable areas for landslide in Kangwondo

Through combining two displacement images, we could find the common displacement areas of different periods. And these regions are expected to be the vulnerable areas for landslide. Figure 5 show these vulnerable areas by red line.

4. CONCLUSION

Through the L-band radar sensor of JERS-1, we could acquire the displacement area of forestry regions in Kangwondo. And we found the vulnerable places for landslide by comparing two different displacement images. The result show various height changes in objective site from centimeter to meter level, and we could detect those change by using 2-pass DInSAR

technique. But we couldn't compare this data with other research or records because JERS-1 had been continuing to observe until 1998 and now, its mission is terminated. However, for the next project of JERS-1, the Japanese National Space Development Agency (NASDA) launched new satellite (Advanced Land Observing Satellite: ALOS) on 2006. It has the same type of L-band sensor like JERS-1, but more improved. So if we use the data of ALOS, it is expected that we can detect the landslide more efficiently than before.

REFRENCE

Goldstein, R. M., H. A. Zebker, and C. L. Werner, 1988, *Satellite radar interferometry: Two-dimensional phase unwrapping, Radio Science*, vol. 23, no. 4, pp. 713-720.

Graham, L. C., 1974, *Synthetic interferometer radar for topographic mapping*, Proc. IEEE, vol. 62, pp. 763-768.

Madsen, S. N., H. A. Zebker, and J. A. Martin, 1993, *Topographic mapping using radar interferometry: Processing techniques*, IEEE Trans. Geosci. Remote Sensing, vol. 31, no 1, pp. 246-256.

Massonnet, D. and K. Fiegl. 1995. "Satellite Radar Interferometric Map of the Coseismic Deformation Field of the M=6.1 Eureka Valley, Calif. Earthquake of May 17, 1993." Geophys. Res. Lett. 22:541-544.

Reigber A, K Papathanassiou, S Cloude, A Moreira, *SAR Tomography and Interferometry for the Remote Sensing of Forested Terrains*, Frequenz, 55, pp 119-123, March/April 2001

Zebker, H. A., S. N. Madsen, J. Martin, K. B. Wheeler, T. Miller, Y. Lou, G. Alberti, S. Vetrella, and A. Cucci, 1991, *The TOPSAR interferometric radar topographic mapping instrument,* IEEE Trans. Geosci. Remote Sensing, vol. 30, no. 5, pp. 933-940.

Zebker, H. A. and J. Villasenor, 1992, *Decorrelation of interferometric radar echoes*, IEEE Trans. Geosci. Remote Sensing, vol. 30, no. 5, pp. 950-959.

Zebker, H. A. and C. Werner, P. A. Rosen, and S. Hensley, 1994, *Accuracy of topographic maps derived from ERS-1 interferometric radar*, IEEE Trans. Geosci. Remote Sensing, vol. 32, no. 4, pp. 823-- 836.

Zebker, H. A., P. A. Rosen, and S. Hensley, 1997, *Atmospheric effects in interferometric synthetic aperture radar surface deformation and topographic maps*, J. Geophys. Res., vol. 102, no. B4, pp. 7547-7563.